analytical chemistry

Article

pubs.acs.org/ac

Highly Sensitive Graphene–Pt Nanocomposites Amperometric Biosensor and Its Application in Living Cell H_2O_2 Detection

Yuanyuan Zhang,[†,‡] Xiaoyun Bai,[‡] Xuemei Wang,*[,†] Kwok-Keung Shiu,*[,‡] Yanliang Zhu,[†] and Hui Jiang[†]

[†]State Key Laboratory of Bioelectronics (Chien-Shiung Wu Laboratory), Southeast University, Nanjing 210096, P. R. China

[‡]Department of Chemistry, Hong Kong Baptist University, Kowloon Tong, Hong Kong

Supporting Information

ABSTRACT: A sensitive hydrogen peroxide (H_2O_2) sensor was constructed based on graphene–Pt (RGO–Pt) nanocomposites and used to measure the release of H_2O_2 from living cells. The graphene and Pt nanoparticles (Pt NPs) were modified on glassy carbon electrode (GCE) by the physical adsorption and electrodeposition of K_2PtCl_6 solution, respectively. Through characterization by scanning electron microscopy (SEM) and energy-dispersive X-ray spectroscopy (EDS), it was observed that the electrodeposited Pt NPs were densely covered and well distributed on the entire graphene surface. Electrochemical study demonstrates that the RGO–Pt nanocomposites modified glassy carbon electrode exhibited a high peak current and low overpotential toward the reduction of H_2O_2. The relevant detection limit of H_2O_2 is ~0.2 μM with a wide linear range from 0.5 μM to 3.475 mM, displaying a much higher sensitivity (459 ± 3 mA M^{-1} cm^{-2}, n = 5) than that of Pt nanoparticles or graphene modified electrode. This novel biosensor can measure the H_2O_2 release from living cells because of its low detection limit, wide linear range, and higher sensitivity.

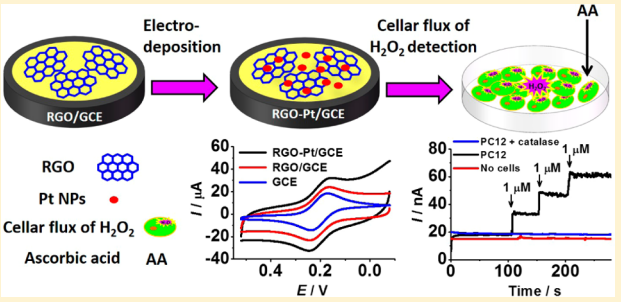

Reactive oxygen species (ROS) are important intracellular signaling molecules, mainly regulating DNA damage, protein synthesis, cell apoptosis, etc.[1−4] However, the excessive amount of ROS accumulation in cells leads to oxidative stress that cause various pathological events such as neurodegeneration, alzheimer disease, autoimmune diseases, and cancer.[5−7] Moreover, it has been proved that ROS at their low concentration can perform as secondary messengers for several growth factors, cytokines, and signal transduction.[1] Therefore, the determination of cellular ROS can lead to a better understanding of the clinical consequences of the enhanced ROS concentration and assist in the studies designed to elucidate the biological effect of ROS in cells. Hydrogen peroxide (H_2O_2) is the most common representative of ROS studied in cellular environments since its long lifetime allows it to penetrate into other cellular compartment to potentially induce various harmful biological modifications. Therefore, selective and quantitative detection of H_2O_2 in cells and measurements of its dynamic release process from living cells are essential to fully understand its roles in cellular physiology and can further provide reliable diagnosis of pathological conditions.[1,2] The fast and accurate detection of H_2O_2 has profound applications in pharmaceutical, clinical, food industry, environmental analysis and other fields.[8,9] Thus, numerous analytical methods have been applied for the detection of H_2O_2 such as fluorescence,[10,11] chemiluminescence,[12,13] and electrochemical methods.[3,4,14−16] Among these methods, the electrochemical technique is most studied because of its simplicity, fast response for analysis, low detection limit, and low costs.[17,18] Sombers and co-workers[3] have detected rapid hydrogen peroxide fluctuations at an uncoated carbon fiber microelectrode by fast scan cyclic voltammetry in vitro and in brain slices with the requisite sensitivity, selectivity, and spatial and temporal resolution. However, the electron-oxidation or electroreduction of H_2O_2 on bare gold or carbon electrode that are extensively used in the electrochemical experiments requires high overpotential (0.5–0.7 V vs Ag/AgCl), while common electroactive species will confuse the measurements.[12,18−20] Therefore, it is important to fabricate chemically modified electrodes lowering the overpotential for the detection of H_2O_2 with high selectivity and sensitivity.

In the past decades, enzyme-based electrochemical biosensors for the detection of H_2O_2 have received considerable attention based on the immobilization of enzymes or proteins in the functionalized electrodes, such as horseradish peroxidase,[8,21] glucose oxidase,[22] cytochrome,[23] and myoglobin.[24] Although the enzyme-based biosensors can acquire remarkable selectivity, however, they are limited by some serious disadvantages, such as environmental instability, high cost, and a complicated immobilization procedure.[8,20,21] Compared with enzymatic sensors, nonenzymatic sensors based on functional nanocomposites have several advantages such as high stability, easy handling, and wide response range.[25−28]

Received: March 17, 2014
Accepted: September 5, 2014
Published: September 5, 2014

   dx.doi.org/10.1021/ac5009699 | *Anal. Chem.* 2014, 86, 9459–9465

Scheme 1. Schematic of the RGO−Pt Modified GCE Used for Detecting H_2O_2 Efflux from Cells Stimulated with Ascorbic Acid (AA)

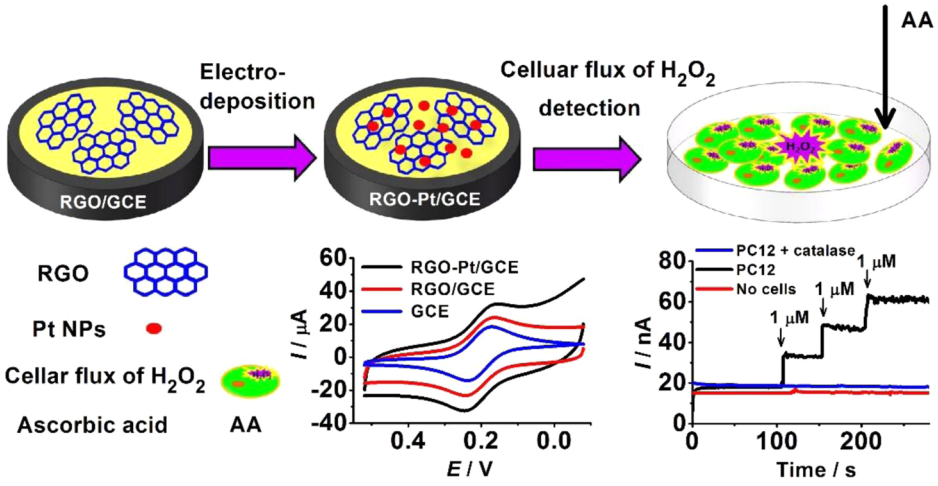

Hence, the nonenzymatic sensors are highly appreciated by the researchers.

Graphene, the isolated two-dimensional carbon nanomaterial, has recently captured tremendous attention in electrochemical biosensing due to its high electron conductivity, large specific surface, fast heterogeneous electron-transfer rate at the graphene sheet edges, and good biocompatibility.[29−32] Graphene was used as a robust scaffold for nanoparticles to form hybrid materials with improved properties. The decoration of graphene with metal nanoparticles can provide larger electrochemically active surface areas and effectively accelerate the electron transfer between electrode and detection molecules leading to a more rapid and sensitive current response.[7,32] Pt nanoparticles (Pt NPs) have high stability and good catalytic performance for H_2O_2 reduction,[33,34] which have been extensively used as an electrode material for the detection of H_2O_2 and fabrication of various biosensors, such as Pt nanoparticles or graphene composites,[33] Pt/ionic liquid/graphene nanocomposite as ascorbic acid and dopamine sensor,[35] and graphene−Pt nanoparticle hybrid material as cholesterol biosensor.[36] Particularly, Pt nanoparticles have been demonstrated to lower the H_2O_2 oxidation/reduction overvoltage efficiently.[19] Therefore, the integration of graphene and Pt NPs possess special features in various applications, that is, catalysis, sensors, optics, electronics, etc.[29] Electrodeposition is a simple and rapid procedure for making nanoparticles that enables fine-tuning and fast response of the nanoparticles to changes in deposition process.[37,38] However, so far it is understood that the electrodeposition of Pt NPs to decorate graphene-modified electrode as a hydrogen peroxide sensor is earlier reported.

In this work, a nonenzymatic H_2O_2 sensor was constructed and used to measure the release of H_2O_2 from living cells (Scheme 1). Reduced graphene oxide (RGO) and Pt nanoparticles (Pt NPs) were modified on glassy carbon electrode (GCE) by physical adsorption and electrodeposition, respectively. The Pt NPs were uniform in particle size and well-dispersed on the graphene surface. The RGO/Pt hybrids modified GCE (RGO−Pt/GCE) has a larger current to the reduction of H_2O_2 than that of the single-component Pt NPs. Considering the low detection limit, wide linear range, and fast response time of biosensor, we can rapidly determine the release of H_2O_2 from living cells (using rat adrenal medulla pheochromocytoma as an example) as potentially useful for physiological and pathological studies.

EXPERIMENTAL SECTION

Reagents and Apparatus. Reduced graphene oxide (RGO) was bought from XF NANO, Inc. (China). Potassium hexachloroplatinate ($K_2PtCl_6{\cdot}6H_2O$) was purchased from Sigma-Aldrich and was used as received. Sodium citrate tribasic dihydrate, β-D(+)glucose, ascorbic acid (AA), and uric acid (UA) were obtained from Sigma. All other chemicals were of reagent-grade and were used as received without any further purification. A 0.02 M phosphate buffer solution (PBS, pH 7.4) comprising NaH_2PO_4 and Na_2HPO_4 was used as the supporting electrolyte. A physiological PBS solution containing KH_2PO_4 (1.76 mM), Na_2HPO_4 (10.14 mM), NaCl (136.75 mM), and KCl (2.28 mM), was mainly used for washing of PC12 cells and observing the release of H_2O_2 from the cells. All the solutions were prepared by doubly distilled water.

The morphological characterizations were obtained with SEM (Electron Microscopy Inc., Cambridge, U.K.). All electrochemical measurements were carried out by a BAS 100BW electrochemical analyzer (Bioanalytical Systems Inc., U.S.A.) and CHI660B electrochemical workstation (CHI Incorporation, U.S.A.) in a conventional three-electrode arrangement, equipped with an Ag/AgCl reference electrode, a platinum wire counter electrode, and a glassy carbon working electrode. All amperometric measurements were regularly carried out in 0.02 M PBS (pH 7.4) with stirring. To get the deoxygenated atmosphere during the experiments, the electrolyte was bubbled with highly purity (99.999%) nitrogen for 20 min and then the electrochemical experiments were performed under inert atmosphere. Anodic current was taken as negative.

Preparation of the Modified Electrodes. RGO suspension of 2 mg/mL was dispersed in doubly distilled water by ultrasonication for 2 h. At first, glassy carbon electrode (GCE, diameter 3 mm) was carefully polished with 0.3 μm Al_2O_3 slurry, and cleaned by brief ultrasonication. Then a certain volume of RGO suspension was cast onto a GCE and dried in air as working electrode; the optimal volume is reported below. Drying time was about 3 h at room temperature. The Pt NPs were deposited by cyclic voltammetry (CV) in the range from −0.4 to +0.6 V at a scan rate of 50 mV/s in 2 mM K_2PtCl_6 solution containing 20 mM HCl; PBS (0.02 M, pH 7.4),

dx.doi.org/10.1021/ac5009699 | Anal. Chem. 2014, 86, 9459−9465

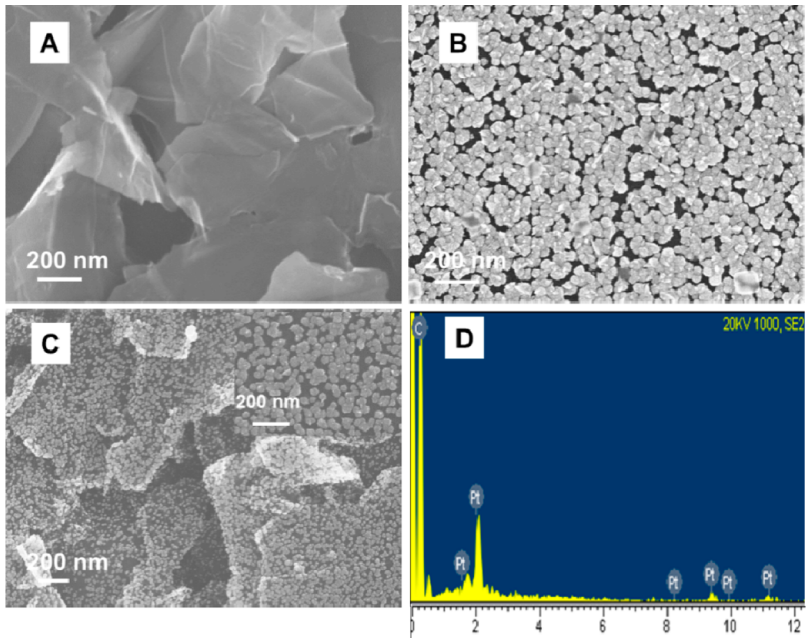

Figure 1. SEM images of RGO (A), Pt NPs (B), and RGO−Pt NPs (C) on GCE. D is the EDS of RGO−Pt nanocomposites.

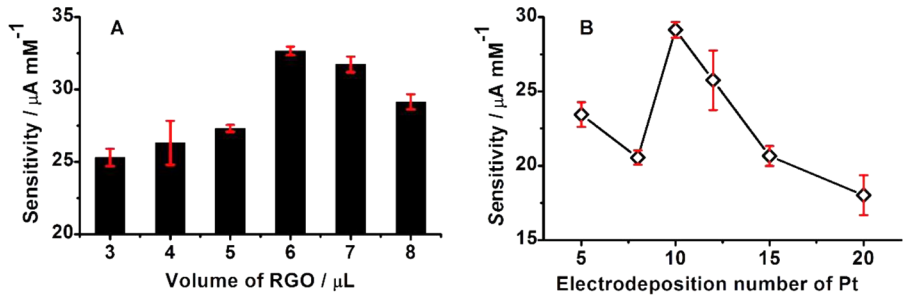

Figure 2. Optimization study on the experimental conditions for the electrocatalytic reduction of H_2O_2. The corresponding responses of the H_2O_2 biosensor through the relevant optimization of RGO volume deposited on the GCE (A) and the CV cycles for electrochemical deposition of Pt NPs on the RGO/GCE (B). Error bars are the standard error of the mean (n = 3 electrodes).

containing NaH_2PO_4 and Na_2HPO_4 was the supporting electrolyte. Then the RGO-Pt/GCE electrode was washed carefully with doubly distilled water to remove the residual K_2PtCl_6 and was allowed to dry at room temperature. The electrolyte solutions were deoxygenated with nitrogen and kept under nitrogen atmosphere during electrochemical studies.

Cell Culture. PC12 (rat adrenal medulla pheochromocytoma) cells were obtained from Institute of Hematology, Chinese Academy of Medical Sciences. They were maintained in DMEM (high glucose, Gibco) medium supplemented with 10% heat-inactivated fetal calf serum (Sigma, USA), 100 U/mL penicillin (Sigma, USA), and 100 mg/mL streptomycin (Sigma, USA) at 37 °C with 5% CO_2 in a 95% humidified atmosphere.

Electrochemical Detection of H_2O_2 Released by Cells. Cells were separated from culture medium by 5 min of centrifugation at 1300 rpm and washed three times with the physiological PBS (0.02 M, pH 7.4) solution. Cell number was estimated by a cell counter. When the current decreased to a level less than 20 nA, ascorbic acid (AA) was injected to the cells suspension, which can motivate cells generation of H_2O_2[39] and have no interference to the detection of H_2O_2. The amperometric current response flux of H_2O_2 in about 6.0×10^6 cells in 2 mL of deoxygenated PBS was recorded at RGO-Pt modified GCE at −0.08 V (vs Ag/AgCl). The experiments were conducted in the water bath at 37 °C.

RESULTS AND DISCUSSION

Characterization of RGO and Pt NPs on Electrode Surface. The TEM images depicted in Figure 1 show the general morphology of the nanomaterials that were used in this study. Single layer structured RGO with smooth surface and size of 200 nm are obtained (Figure 1A). Figure 1B depicts the Pt NPs electrodeposited on the GCE with the size of 40 nm. From Figure 1C and Figure 1D, it can be observed that there are lots of Pt NPs densely covered and well distributed on the entire graphene surfaces to form the RGO−Pt blending nanocomposites (i.e., EDS indicates that their main composites are C and Pt elements), that are believed to be capable of enhancing the relevant electrochemical detection.

Optimization Study of RGO−Pt Nanocomposite-Modified Electrodes. Our observations indicate that the deposition volume of RGO shows an important effect on the sensitivity of the H_2O_2 biosensor. The sensitivity response increased with the increasing volume of deposition and reached a summit at a volume of 6 μL of RGO (2.0 mg/mL), afterward it decreased upon addition of much larger deposition volume (Figure 2A). The deposition dosage of Pt NPs on the electrode

dx.doi.org/10.1021/ac5009699 | Anal. Chem. 2014, 86, 9459−9465

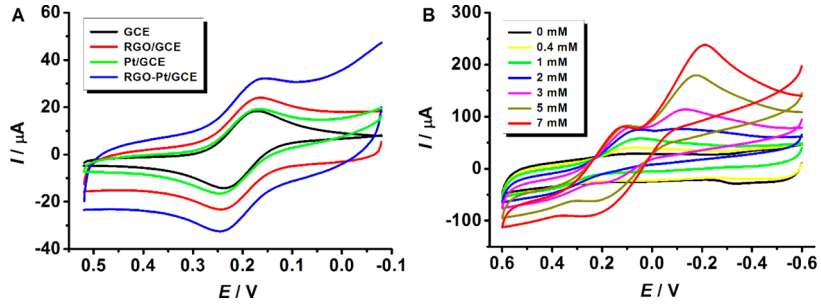

Figure 3. (A) CV study of potassium ferricyanide solution containing 0.1 M KCl and 1 mM $K_3[Fe(CN)_6]$ on the bare GCE, RGO/GCE, and RGO−Pt/GCE. Scan rate: 100 mV/s. (B) Typical CV curves of RGO-Pt/GCE in the presence of H_2O_2, where H_2O_2 concentrations in 0.02 M PBS solution (pH 7.4) are 0, 0.4, 1, 2, 3, 5, and 7 mM. Scan rate: 100 mV/s.

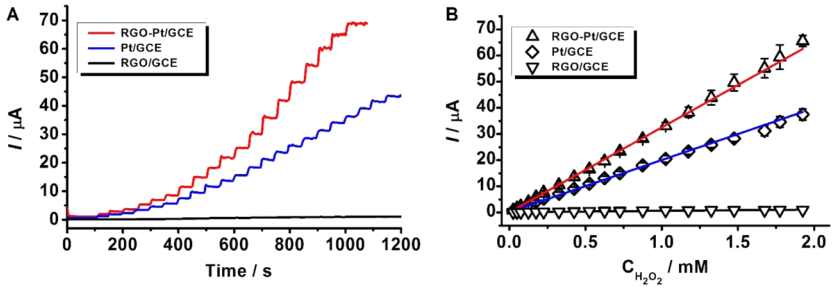

Figure 4. (A) Amperometric *i*−*t* curves of RGO−Pt/GCE, Pt/GCE, and RGO/GCE in N_2-saturated PBS (0.02 M, pH 7.4) at −0.08 V with successive addition of H_2O_2. (B) Corresponding calibration curves of current versus H_2O_2 concentrations for RGO−Pt/GCE, Pt/GCE, and RGO/GCE. Error bars are the standard error of the mean (n = 5 electrodes).

has also been optimized since low Pt deposit can lead to low coverage and thus poor catalysis, while high dosage of Pt deposit will lead to low catalytic efficiency and higher aggregation. When the number of CV cycles employed for electrochemical deposition was ten, the sensitivity response to H_2O_2 detection reached a maximum (Figure 2B). Therefore, 6 μL of RGO (2.0 mg/mL) and 10 CV cycles for Pt NPs deposition were used in the experiment.

Electrocatalytic Reduction of H_2O_2 on RGO−Pt Nanointerface. To investigate the electrocatalytic performance of the RGO−Pt nanocomposites for H_2O_2 reduction, a nonenzymatic sensor was fabricated through the RGO−Pt nanocomposites modified glassy carbon electrode (RGO−Pt/GCE). Initially, the surface area of modified electrodes were measured in 1 mM $K_3[Fe(CN)_6]$ solution containing 0.1 M KCl. As shown in Figure 3A, a pair of well-defined oxidation and reduction peaks owing to the $[Fe(CN)_6]^{3-/4-}$ redox couple was exhibited. According to the Randled−Sevcik equation[40]

$$I_p = 2.69 \times 10^5 A D^{1/2} n^{3/2} \gamma^{1/2} C$$

where A is the area of the electroactive surface area (cm^2), D is the diffusion coefficient of the molecule in solution ($6.70 \pm 0.02 \times 10^{-6}$ cm^2 s^{-1}), n is the number of electrons participating in the redox reaction (for $[Fe(CN)_6]^{3-/4-}$, n = 1), γ is the scan rate of the potential perturbation (V s^{-1}), and C is the bulk concentration of the redox probe (mol cm^{-3}). The surface area of electrodes were calculated in the trend of bare GCE (0.07065 cm^2) < Pt/GCE (0.0777 cm^2) < RGO/GCE (0.0801 cm^2) < RGO−Pt/GCE (0.0847 cm^2), suggesting that RGO−Pt nanocomposites can enlarge the surface area because of its three-dimensional structure and Pt NPs uniformly distributed on the RGO surface.

RGO−Pt nanocomposites are favorable for the unlimited transport of molecules and electron conductivity because of the particularly desirable three-dimensional bicontinuous skeleton and uniformly distributed nanoparticles (Figure 1). Thus, it is interesting to explore the electrocatalytic activity of H_2O_2 electroreduction over the RGO−Pt nanocomposites. Figure 3B shows the CV curves of RGO−Pt/GCE in 0.02 M PBS solution (pH 7.4) in the absence and presence of H_2O_2. As shown in Figure 3B, a reduction peak emerges in the presence of 0.4 mM H_2O_2 and slightly shifts to negative potentials with increasing H_2O_2 concentration, presumably due to the sluggish electron transfer kinetics.[18] The reduction current around −0.1 V dramatically increases with increasing H_2O_2 concentration, indicating that H_2O_2 can be easily reduced on these RGO−Pt nanostructures over a broad concentration range. The remarkable electrocatalytic activity of RGO−Pt/GCE can be attributed to the unique nanostructures, high surface-to-volume ratio, and the synergistic effects provided by RGO and Pt nanoparticles which is of significance for highly selective and sensitive detection of H_2O_2.

Amperometric Response and Calibration Curve for H_2O_2 Detection. The detection sensitivity on the relevant modified electrodes was further explored through amperometric study. Three differnet potentials (−0.1, −0.08, and 0 V) were chosen for the amperometric examination (Supporting Information Figure S1). The response to H_2O_2 was the highest at an applied potiential of −0.08 V. As shown in Figure 4, the response for the successive injection of different amounts of H_2O_2 and the typical *i*−*t* curves at −0.08 V were displayed. It is evident that RGO−Pt/GCE exhibited enhanced amperometric response for H_2O_2 detection compared with Pt/GCE and RGO/GCE. The steady-state current of RGO−Pt/GCE could reach 95% within 5 s after the injection of H_2O_2 (the red curve, Figure 4A). However, no clear response or only weak signal was obtained on the RGO/GCE (the black curve) and Pt/GCE (the blue curve), respectively. The corresponding current−

dx.doi.org/10.1021/ac5009699 | Anal. Chem. 2014, 86, 9459−9465

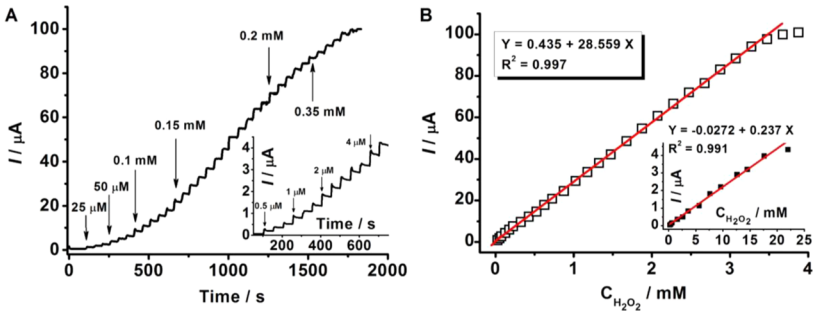

Figure 5. (A) Amperometric $i-t$ curves of RGO−Pt/GCE in N_2-saturated PBS (0.02 M, pH 7.4) at −0.08 V with successive addition of H_2O_2 0.025, 0.05, 0.1, 0.15, 0.2, and 0.35 mM (H_2O_2 was added at the points indicated by arrows to the concentrations mentioned in (A)). Inset: $i-t$ curve shows the response of RGO−Pt/GCE to H_2O_2 with successive addition of H_2O_2 0.5, 1.0, 2.0, and 4.0 μM. (B) Corresponding calibration curves with H_2O_2 concentrations ranging from 0.025 to 3.475 mM. Inset: Calibration curves with H_2O_2 concentrations ranging from 0.5 to 22.5 μM.

Table 1. Comparison of the Performance of Various Hydrogen Peroxide Sensors

electrode materials	detection potential (V)	linear range (μM)	detection limit (μM)	ref
graphene/Au nanoparticles/toluidine blue O films	−0.3 (vs SCE)	5−25362	0.2	2
Pt/graphene-nanocomposite	−0.2 (vs SCE)	2.5−6650	0.8	7
Pt/carbon nanotube nanocomposite	−0.1 (vs Ag/AgCl)	5−25000	1.5	20
cytochrome/microporous carbon electrode	−0.033 (vs SCE)	20−240	14.6	23
myoglobin/chitosan/lanthanum-substituted bismuth titanate-nanocomposite	−0.28 (vs Ag/AgCl)	2−490	0.14	24
graphene/Pt-nanocomposite	0 (vs Ag/AgCl)	2−710	0.5	33
Se/Pt-nanocomposites	0 (vs SCE)	10−15000	3.1	34
Pt nanoparticle-loaded carbon nanofiber electrode	0 (vs Ag/AgCl)	1−800	0.6	41
PtAu/graphene-sheets-multi walled carbon nanotubes	−0.47 (vs SCE)	2−8561	0.6	42
mesoporous platinum microelectrode	0.6 (vs SCE)	20−40000	4.5	43
graphene/Pt-nanocomposite	−0.08 (vs Ag/AgCl)	0.5−3475	0.2	this work

concentration calibration plots in Figure 4B also clearly show that the RGO−Pt/GCE displays a significantly enhanced sensitivity, and a linear relationship is established in the range of 0.025−2 mM with a correlation coefficient of R^2 = 0.998. The linear equation is I (μA) = 32.45C + 0.07 (where C is the concentration of H_2O_2) for RGO−Pt/GCE with a sensitivity of 459 ± 3 mA M^{-1} cm^{-2} based on n = 5 electrodes. While for Pt/GCE the linear relationship is I (μA) = 19.88C + 0.17 with a sensitivity of 281 ± 4 mA M^{-1} cm^{-2} based on n = 4 electrodes. These results further reveal the excellent performance of RGO−Pt as a promising material in H_2O_2 detection. As shown in Figure 5, the relevant linear range for the detection of H_2O_2 at the applied potential of −0.08 V contained two segments: 0.5 × 10^{-6}−2.25 × 10^{-5} M (correlation coefficient R^2 = 0.991) and 2.5 × 10^{-5}−3.475 × 10^{-3} M (correlation coefficient R^2 = 0.997). The detection limit for the H_2O_2 sensor is estimated to be ∼0.2 μM (ratio of signal-to-noise S/N = 3). A comparison of detection potential, linear range, and detection limit for RGO−Pt/GCE with other H_2O_2 sensors reported in the literature are shown in Table 1, indicating that the analytical parameters for RGO−Pt/GCE are comparable and even better than those obtained at several electrodes reported recently. Therefore, the RGO−Pt nanointerface is excellent as the promising candidate for H_2O_2 amperometric sensor with a wide linear range, low detection potential, and high sensitivity.

The potential interference of electroactive compounds in physiological fluid at the RGO−Pt/GCE was extensively examined. Figure 6 illustrates the amperometric response of the relevant sensor upon addition of 0.1 mM H_2O_2, 1.0 mM uric acid (UA), 0.5 mM AA, 1.0 mM glucose (GLU), and a second injection of 0.1 mM H_2O_2. UA, AA, and GLU yielded little current response at the RGO−Pt/GCE under the applied

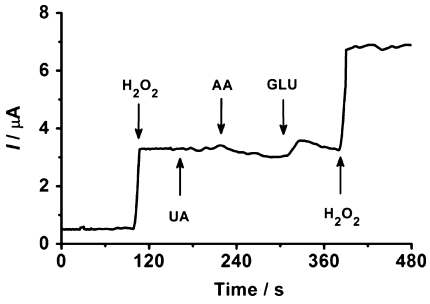

Figure 6. Amperometric $i-t$ response of RGO−Pt/GCE at −0.08 V in N_2-saturated PBS (0.02 M, pH 7.4) to successive addition of 0.1 mM H_2O_2, 1.0 mM UA, 0.5 mM AA, 1.0 mM GLU, and a second 0.1 mM H_2O_2.

negative potential. The current response of 0.1 mM H_2O_2 was also not affected in the presence of the other compounds. The low potential (−0.08 V) applied for detection endowed the sensor with high selectivity.

Long-term stability and reproducibility is quite essential for nanomaterials modified electrode to construct the sensor. Six independently RGO−Pt/GCE showed a good reproductivity with a deviation less than 4.5% (RSD) for the sensitivity to H_2O_2. When the as-prepared RGO−Pt/GCE was stored at room temperature, the sensitivity response to H_2O_2 declined to ∼81% within 2 weeks and kept steady (shown as Supporting Information Figure S2). Our results further suggest the reliability of the RGO−Pt modified electrode for determination of H_2O_2 since these electrodes display excellent combination of low detection potential, wide linear range, and high sensitivity.

Measurements of H_2O_2 Release from Living Cells. The detection of H_2O_2 in living cells was performed to explore the

dx.doi.org/10.1021/ac5009699 | Anal. Chem. 2014, 86, 9459−9465

application of the RGO−Pt electrode. H_2O_2 plays important roles in many biological processes,[1,44] and thus quantitative detection of H_2O_2 distribution and the in situ dynamic release processes in cells are essential. The dynamic H_2O_2 release in rat adrenal medulla pheochromocytoma PC12 cells were monitored using the as-prepared RGO−Pt/GCE and stimulated by injecting AA to induce H_2O_2 generation in cells.[1,2] Figure 7

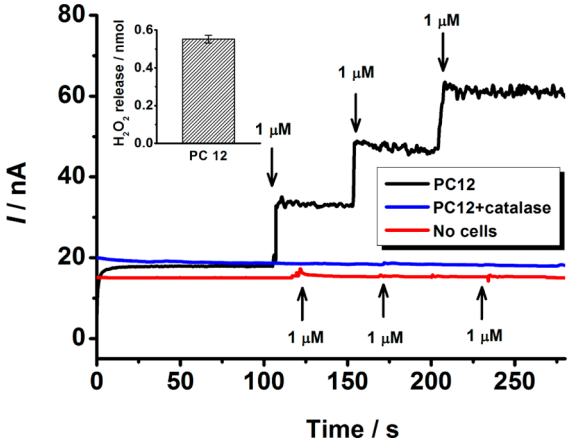

Figure 7. Time course of the H_2O_2 release from PC 12 cells upon the successive addition of 1 μM AA. The red line is for the experiment without cells; the blue line is for the experiment PC12 cells and 300 U/mL catalases. Inset: The release of H_2O_2 from 6.0×10^6 cells in 2 mL of deoxygenated PBS upon injection of 3 μM AA. The values are based on at least three independent measurements.

shows the amperometric response curve of the RGO−Pt/GCE in the presence of PC12 cells triggered by different amounts of AA in physiological PBS buffer at −0.08 V versus Ag/AgCl. As a control, the buffer solution without the cells (red line, Figure 7) and the cells with catalase (blue line, Figure 7) under the same conditions were also measured and no current change was observed. With the PC12 cells, the current was increased significantly according to successive addition of AA, and the current reached a maximum in a few seconds. However, when 300 U/mL catalase was added in advance to the PBS the current remained nearly constant (blue line, Figure 7). These results are consistent with the earlier reports.[2] The constant current response should be due to the specific disintegration of H_2O_2 released from PC12 cells by catalase upon the stimulation of AA.[2] The release rates of H_2O_2 are dependent on the AA concentration as indicated by the slopes of the curves after each injection. The maximum current of ~46.9 nA upon injection of 3 μM AA roughly corresponds to a H_2O_2 concentration of 0.313 μM in cell solution, according to the standard curve shown in Figure 5B inset. The cell solution was of 2 mL, corresponding to 0.63 ± 0.02 nmol of H_2O_2 released from cells. The number of cells used in the measurements were about 6.0×10^6, and the H_2O_2 released from each cell was about 105 ± 3.3 amol, as reported earlier.[1−3] These results also suggest that the RGO−Pt/GCE can be used for the detection of H_2O_2 release from cells and its potential uses can be exploited for physiological and pathological studies.

The possible rational behind the production and release of H_2O_2 in cells stimulated by AA may be attributed to the following points. In general, the concentration of H_2O_2 in cells keeps a value favored for cellular proliferation, while the process to maintain redox homeostasis inside cells is conducted not only by catabolism but also by excretion of H_2O_2.[2,45] It is already observed that H_2O_2 can readily cross the lipid bilayer of membrane.[46] However, some researches declared that H_2O_2 could permeate across biomembranes rapidly and the diffusion was facilitated by some channel proteins, such as aquaporins.[45,47] In any case, the relevant H_2O_2 can diffuse from high to low concentration regions when intracellular redox homeostasis was interrupted by artificial stimulation, hence the extracellular and intracellular concentrations of H_2O_2 were regulated to remain at the same level. Thus, this raises the possibility of the in situ quantitative detection of the flux of H_2O_2 from living cells for further evaluation of oxidative stress in cells.

CONCLUSION

In summary, a nonenzymatic H_2O_2 sensor was fabricated in this study based on RGO−Pt nanocomposites with high Pt nanoparticles loading. Electrochemical investigation indicated that the RGO−Pt-modified electrode exhibited much better catalysis and higher sensitivity for H_2O_2 detection than that based on single component. The observations demonstrate that the RGO−Pt nanocomposites on modified glass carbon electrode exhibited a high peak current and low overpotential toward the reduction of H_2O_2. The relevant detection limit of H_2O_2 was ~0.2 μM, with a wide linear range from 0.5 μM to 3.475 mM. These results indicate that the RGO−Pt nanocomposites can provide a promising platform for the study of graphene based composites in electrocatalysis and electrochemical biosensing of H_2O_2 with high sensitivity. Moreover, RGO−Pt electrode provides an enzyme-free electrode for the detection of H_2O_2 in living cells because of the good electrocatalytic activity, facile preparation, and higher stability.

ASSOCIATED CONTENT

Supporting Information

Additional information as noted in text. This material is available free of charge via the Internet at http://pubs.acs.org.

AUTHOR INFORMATION

Corresponding Authors

*E-mail: xuewang@seu.edu.cn. Tel.: +86-25-83792177.
*E-mail: kkshiu@hkbu.edu.hk. Tel.: +852 3411 7346.

Notes

The authors declare no competing financial interest.

ACKNOWLEDGMENTS

This work is supported by the National Basic Research Program (2010CB732404), National Science Foundation of China (81325011, 21175020), the National High Technology Research and Development Program of China (2012AA022703), Suzhou Science & Technology Major Project (ZXY2012028), and the Faculty Research Grants of HKBU (FRG2/11-12/078).

REFERENCES

(1) Zhang, Y.; Wu, C.; Zhou, X.; Wu, X.; Yang, Y.; Wu, H.; Guo, S.; Zhang, J. *Nanoscale* **2013**, *5*, 1816−1819.
(2) Chang, H.; Wang, X.; Shiu, K.-K.; Zhu, Y.; Wang, J.; Li, Q.; Chen, B.; Jiang, H. *Biosens. Bioelectron.* **2013**, *41*, 789−794.
(3) Sanford, A. L.; Morton, S. W.; Whitehouse, K. L.; Oara, H. M.; Lugo-Morales, L. Z.; Sombers, L. A. *Anal. Chem.* **2010**, *82*, 5205−5210.
(4) Roberts, J. G.; Hamilton, K. L.; Sombers, L. A. *Analyst* **2011**, *136*, 3550−3556.

(5) Wu, P.; Cai, Z.; Gao, Y.; Zhang, H.; Cai, C. *Chem. Commun.* **2011**, *47*, 11327−11329.
(6) Trachootham, D.; Alexandre, J.; Huang, P. *Nat. Rev. Drug Discovery* **2009**, *8*, 579−591.
(7) Pagliari, F.; Mandoli, C.; Forte, G.; Magnani, E.; Pagliari, S.; Nardone, G.; Licoccia, S.; Minieri, M.; Di Nardo, P.; Traversa, E. *ACS Nano* **2012**, *6*, 3767−3775.
(8) Yao, S.; Xu, J.; Wang, Y.; Chen, X.; Xu, Y.; Hu, S. *Anal. Chem. Acta* **2006**, *557*, 78−84.
(9) Zhang, F.; Wang, F.; Zhang, Y.; Zheng, Z.; Wang, C.; Du, Y.; Ye, W. *Int. J. Electrochem. Sci.* **2012**, *7*, 1968−1977.
(10) Wen, F.; Dong, Y.; Feng, L.; Wang, S.; Zhang, S.; Zhang, X. *Anal. Chem.* **2011**, *83*, 1193−1196.
(11) Hirakawa, K. *Anal. Bioanal. Chem.* **2006**, *386*, 244−248.
(12) Wang, K.; Liu, Q.; Wu, X.-Y.; Guan, Q.-M.; Li, H. N. *Talanta* **2010**, *82*, 372−376.
(13) Tahirović, A.; Čopra, A.; Omanović-Mikličanin, E.; Kalcher, K. *Talanta* **2007**, *72*, 1378−1385.
(14) Hua, M.-Y.; Chen, H.-C.; Chuang, C.-K.; Tsai, R.-Y.; Jeng, J.-L.; Yang, H.-W.; Chern, Y.-T. *Biomaterials* **2011**, *32*, 4885−4895.
(15) Zhang, J.-J.; Liu, Y.-G.; Jiang, L.-P.; Zhu, J.-J. *Electrochem. Commun.* **2008**, *10*, 355−358.
(16) Li, J.; Li, Y.; Zhang, Y.; Wei, G. *Anal. Chem.* **2012**, *84*, 1888−1893.
(17) Xu, S.; Peng, B.; Han, X. *Biosens. Bioelectron.* **2007**, *22*, 1807−1810.
(18) Chakraborty, S.; Retna Raj, C. *Biosens. Bioelectron.* **2009**, *24*, 3264−3268.
(19) Chu, X.; Duan, D.; Shen, G.; Yu, R. *Talanta* **2007**, *71*, 2040−2047.
(20) Wen, Z.; Ci, S.; Li, J. *J. Phys. Chem. C* **2009**, *113*, 13482−13487.
(21) Liu, X.; Feng, H.; Zhang, J.; Zhao, R.; Liu, X.; Wong, D. K. *Biosens. Bioelectron.* **2012**, *32*, 188−194.
(22) Wang, H.; Lang, Q.; Li, L.; Liang, B.; Tang, X.; Kong, L.; Mascini, M.; Liu, A. *Anal. Chem.* **2013**, *85*, 6107−6112.
(23) Zhang, L. *Biosens. Bioelectron.* **2008**, *23*, 1610−1615.
(24) Hu, J.; Yu, Y.; Guo, H.; Chen, Z.; Li, A.; Feng, X.; Xi, B.; Hu, G. *J. Mater. Chem.* **2011**, *21*, 5352−5359.
(25) López-Lorente, A.; Simonet, B.; Valcárcel, M. *Anal. Bioanal. Chem.* **2011**, *399*, 43−54.
(26) Batchelor-McAuley, C.; Du, Y.; Wildgoose, G. G.; Compton, R. G. *Sens. Actuators, B* **2008**, *135*, 230−235.
(27) Park, S.; Chung, T. D.; Kim, H. C. *Anal. Chem.* **2003**, *75*, 3046−3049.
(28) Meng, L.; Jin, J.; Yang, G.; Lu, T.; Zhang, H.; Cai, C. *Anal. Chem.* **2009**, *81*, 7271−7280.
(29) Guo, S.; Dong, S.; Wang, E. *ACS Nano* **2009**, *4*, 547−555.
(30) Bai, J.; Jiang, X. *Anal. Chem.* **2013**, *85*, 8095−8101.
(31) Wu, S.; He, Q.; Tan, C.; Wang, Y.; Zhang, H. *Small* **2013**, *9*, 1160−1172.
(32) Pumera, M. *Chem. Soc. Rev.* **2010**, *39*, 4146−4157.
(33) Xu, F.; Sun, Y.; Zhang, Y.; Shi, Y.; Wen, Z.; Li, Z. *Electrochem. Commun.* **2011**, *13*, 1131−1134.
(34) Li, Y.; Zhang, J.-J.; Xuan, J.; Jiang, L.-P.; Zhu, J.-J. *Electrochem. Commun.* **2010**, *12*, 777−780.
(35) Li, F.; Chai, J.; Yang, H.; Han, D.; Niu, L. *Talanta* **2010**, *81*, 1063−1068.
(36) Dey, R. S.; Raj, C. R. *J. Phys. Chem. C* **2010**, *114*, 21427−21433.
(37) Guo, S.; Wang, L.; Wang, E. *Chem. Commun.* **2007**, 3163−3165.
(38) Zhang, H.; Xu, J.-J.; Chen, H.-Y. *J. Phys. Chem. C* **2008**, *112*, 13886−13892.
(39) Chen, Q.; Espey, M. G.; Krishna, M. C.; Mitchell, J. B.; Corpe, C. P.; Buettner, G. R.; Shacter, E.; Levine, M. *Proc. Natl. Acad. Sci. U. S. A.* **2005**, *102*, 13604−13609.
(40) Yang, M.; Yang, Y.; Liu, Y.; Shen, G.; Yu, R. *Biosens. Bioelectron.* **2006**, *21*, 1125−1131.
(41) Liu, Y.; Wang, D.; Xu, L.; Hou, H.; You, T. *Biosens. Bioelectron.* **2011**, *26*, 4585−4590.
(42) Lu, D.; Zhang, Y.; Lin, S.; Wang, L.; Wang, C. *Talanta* **2013**, *112*, 111−116.
(43) Evans, S. A.; Elliott, J. M.; Andrews, L. M.; Bartlett, P. N.; Doyle, P. J.; Denuault, G. *Anal. Chem.* **2002**, *74*, 1322−1326.
(44) Rhee, S. G. *Science* **2006**, *577*, 1882−1883.
(45) Bienert, G. P.; Schjoerring, J. K.; Jahn, T. P. *Biochim. Biophys. Acta* **2006**, *1758*, 994−1003.
(46) Jones, R. D.; Morice, A. H. *Pharmacol. Ther.* **2000**, *88*, 153−161.
(47) Bienert, G. P.; Møller, A. L.; Kristiansen, K. A.; Schulz, A.; Møller, I. M.; Schjoerring, J. K.; Jahn, T. P. *J. Biol. Chem.* **2007**, *282*, 1183−1192.